Commun Nonlinear Sci Numer Simulat 85 (2020) 105258

Contents lists available at ScienceDirect

Commun Nonlinear Sci Numer Simulat

journal homepage: www.elsevier.com/locate/cnsns

Research paper

Time-frequency analysis of a new aperiodic resonance

Jianhua Yang[a,b,*], Shuai Zhang[a,b], Miguel A.F. Sanjuán[c,d], Houguang Liu[a,b]

[a] School of Mechatronic Engineering, China University of Mining and Technology, Xuzhou 221116, PR China
[b] Jiangsu Key Laboratory of Mine Mechanical and Electrical Equipment, China University of Mining and Technology, Xuzhou 221116, PR China
[c] Nonlinear Dynamics Chaos and Complex Systems Group Departamento de Física, Universidad Rey Juan Carlos, Tulipán s/n 28933, Móstoles, Madrid, Spain
[d] Department of Applied Informatics, Kaunas University of Technology, Studentu 50-407, Kaunas 51368, Lithuania

ARTICLE INFO

Article history:
Received 9 December 2019
Revised 14 February 2020
Accepted 13 March 2020
Available online 14 March 2020

Keywords:
Aperiodic resonance
Optimization algorithm
Nonlinear frequency modulated signal
Signal enhancement

ABSTRACT

Based on the time-frequency analysis, a piecewise re-scaled method is proposed to realize aperiodic resonance in a Duffing system excited by the nonlinear frequency modulated (NLFM) signal. Based on the aperiodic resonance theory, the weak NLFM signal is enhanced greatly. By short time Fourier transform, numerical simulations are carried out for several kinds of NLFM signal. The results show that the method enhances the NLFM signal effectively. Meanwhile, the effectiveness of the method is still illustrated in the noise background. In addition, the noise and the interference frequency can be removed. Noteworthy, and differently as what happens with the stochastic resonance and vibrational resonance, the aperiodic resonance does not require any auxiliary signal or noise to induce it. This constitutes also a new result of this paper. Next, in order to expand the application of this method, it is used to process the experiment signal of bearing fault under variable speed condition. The validity of the method is illustrated again. The results provide new reference in processing non-stationary frequency-modulated signal. Finally, an adaptive piecewise re-scaled aperiodic resonance scheme is put forward to get optimal parameters to induce stronger aperiodic resonance quickly.

1. Introduction

Signal is usually considered as a representation of the operating state of an equipment or a system. However, in the actual signal acquisition process, the target signal usually contains a large number of interference components due to the existence of complex working conditions. These interference components make the target signal extremely weak and difficult to identify. Therefore, the signal enhancement methods have attracted more and more attention in various fields, such as acoustics [1], chemistry [2], biology [3], optics [4–6], and fault diagnosis [7–9].

Frequency modulated signal is a kind of typical signal [10–13], which is widely used in science and engineering. In particular, the processing of nonlinear frequency modulation (NLFM) signal has attracted increasing attention, such as in the field of radar [14,15], communication engineering [16,17], etc. Therefore, the study of NLFM signal is particularly important in engineering application. At present, some time-frequency analysis techniques have been used to process frequency-modulated

* Corresponding author.
E-mail address: jianhuayang@cumt.edu.cn (J. Yang).

https://doi.org/10.1016/j.cnsns.2020.105258
1007-5704/

signal. Such as the time-varying demodulation analysis [18], the variational mode decomposition [19], the generalized synchrosqueezing transform [20], the wavelet analysis [21] and so on. In addition, the enhancement of weak frequency modulation signal has achieved some research results [22,23], especially in the field of mechanical fault detection [24,25].

Nowadays, some nonlinear resonance methods have been widely used to enhance the weak signal. For example, both stochastic resonance (SR) [26] and vibrational resonance (VR) [27] can produce a signal enhancement. When SR occurs, the noise in the output is suppressed and the weak signal is enhanced. SR method has been applied to the detection of weak signal [28-31]. In fact, even if the optimal SR output can be obtained adaptively, there are still some extra interference frequency components due to the existence of random excitation. Moreover, the signal-to-noise ratio often cannot be greatly improved by SR method. VR is another effective method to enhance weak characteristic signal [32,33], which is similar in a certain sense to SR method. The main difference is that the noise is substituted by a fast auxiliary excitation. However, compared with the noise, a fast excitation in determined form is easier to control. Therefore, the application of VR method has also achieved some results in weak characteristic signal enhancement [34]. Nevertheless, VR method has a few drawbacks, such as the distortion between the time domain waveform of the system output and the original signal. SR and VR methods use noise or auxiliary signal to induce resonance phenomenon, so as to realize the purpose of signal enhancement. However, there is few work on using aperiodic signal directly to induce aperiodic resonance and enhance aperiodic signal, especially for NLFM signal. Due to the frequency of the NLFM signal is time modulated, to realize the aperiodic resonance is much more difficult than SR and VR. Therefore, the research motivation of this paper is the new nonlinear dynamic phenomenon and the application of aperiodic resonance.

In a nonlinear system excited by a single signal only, the response may present complex resonance phenomenon. At this point, the weak signal would be enhanced greatly when strong resonance occurs at the characteristic frequency. With regard to a NLFM signal excited system, the resonance may also appear under certain conditions. Considering the frequency is modulated with the time, the conditions of the strong resonance may be difficult to obtain. Motivated by this problem, we try to propose the piecewise re-scaled method to induce strong resonance in a simple Duffing system and enhance the NLFM signal to a great extent.

The rest of the paper is organized as follows. In Section 2, the theoretical formulation of the piecewise re-scaled aperiodic resonance method is introduced in detail. In Section 3, the feasibility of this method is verified by using several kinds of NLFM signal. In Section 4, the proposed method is applied to process the experimental signal of bearing fault. In Section 5, the adaptive piecewise re-scaled aperiodic resonance method is proposed by using an optimization algorithm to find out the optimal system parameters quickly. In the last section, the main conclusions of the paper are given.

2. Piecewise re-scaled method

The second-order Duffing system is governed by the following differential equation

$$\frac{\mathrm{d}^2x}{\mathrm{d}t^2} + \delta\frac{\mathrm{d}x}{\mathrm{d}t} - ax + bx^3 = s(t) \tag{1}$$

The system parameters $a>0$, $b>0$, and δ is the damping coefficient. Here, as an example of NLFM signal, the function $s(t)$ is described by

$$s(t) = s_1(t) = A\cos\left(\pi\gamma t^3 + 2\pi f_0 t + \varphi\right), \tag{2}$$

where A, γ, f_0 and φ are the amplitude, the chirp rate, the carrier frequency and the initial phase of the NLFM signal, respectively.

A small excitation amplitude can be enhanced due to the existence of a nonlinear resonance. The resonance condition may be achieved by tuning the system parameters appropriately. Then, it further induces the aperiodic resonance to enhance the weak external excitation signal.

Differentiating the phase of the NLFM signal, the instantaneous frequency $f(t)$ is obtained

$$f(t) = 3\pi\gamma t^2 + 2\pi f_0 \tag{3}$$

Obviously, the instantaneous frequency is a nonlinear function of the time. What we need to point out is that if we choose heterz (Hz) as the unit of the frequency, the instantaneous frequency is $\frac{1}{2\pi}f(t)$.

With the increase of time, according to Eq. (3), the frequency of the external excitation signal also increases gradually. At this point, it is difficult to achieve the aperiodic resonance and get the optimal enhancement effect. In order to enhance the NLFM signal by an aperiodic resonance, the idea of signal segmenting was introduced in our former works [35]. By dividing the whole signal into several sections, searching for the system parameters to match the frequency of the excitation in each segmentation, a resonance response is achieved respectively corresponding to each output. In this process, getting different system parameters to match each signal segmentation is the key step. The frequency of the NLFM signal increase continuously over time, the “high-frequency” should be processed. There are some methods to solve this problem, such as the normalized scale transformation method [36], the twice-sampling method [37], the frequency-shifted and re-scaling method [38,39], etc. These methods help us to find the system parameters that approximately matching the signal frequency and then realize the aperiodic resonance. The general scale transformation method is a better method and it can achieve a stronger resonance [40]. As a result, it is used to process the NLFM signal in this subsection. Hence, for the signal processing,

we have three steps. First, the whole NLFM signal is segmented into several sections. Second, each segmentation is consider as an input to get the output. All these outputs in turn constitute the whole response of the system. Finally, the resonance of each segmentation is achieved by choosing different appropriate system parameters.

The re-scaled parameter m is defined as

$$m = m_0\left(3\pi\gamma {t_{ei}}^2 + 2\pi f_0\right) \tag{4}$$

where m_0 is a fundamental scale coefficient. t_{ei} represents the time corresponding to the end point of the ith signal segmentation. We use d as the number of segmentation. In a different segmentation, we may have a different rescaled-parameter m.

Then, we introduce the variables

$$x(t) = z(\tau), \tau = mt \tag{5}$$

Substituting Eq. (5) into Eq. (1), we get

$$\frac{\mathrm{d}^2 z(\tau)}{\mathrm{d}\tau^2} + \frac{\delta}{m}\frac{\mathrm{d}z(\tau)}{\mathrm{d}\tau} - \frac{a}{m^2}z(\tau) + \frac{b}{m^2}z^3(\tau) = \frac{1}{m^2}s\left(\frac{\tau}{m}\right) \tag{6}$$

Now, if we define

$$\frac{a}{m^2} = a_1, \frac{b}{m^2} = b_1, \frac{\delta}{m} = \delta_1 \tag{7}$$

we have

$$\frac{\mathrm{d}^2 z(\tau)}{\mathrm{d}\tau^2} + \delta_1\frac{\mathrm{d}z(\tau)}{\mathrm{d}\tau} - a_1 z(\tau) + b_1 z^3(\tau) = \frac{1}{m^2}s\left(\frac{\tau}{m}\right) \tag{8}$$

According to Eq. (8), the external excitation frequency is reduced to $1/m$ of the frequency of the original signal. Meanwhile, a_1 and b_1 are system parameters by the excitation of the low-frequency signal. Further, the input signal is restored to its original strength by the following formula,

$$\frac{\mathrm{d}^2 x}{\mathrm{d}t^2} + m\delta_1\frac{\mathrm{d}x}{\mathrm{d}t} - m^2 a_1 x + m^2 b_1 x^3 = m^2 s(t) \tag{9}$$

In Eq. (9), by choosing an appropriate value of m, an aperiodic resonance at an arbitrary excitation frequency may be realized. The enhanced segmentation with small amplitude may be submerged by that with large amplitude. Therefore, for all segmented signals, the same parameters a_1, b_1 and m_0 are selected to avoid this situation.

In order to measure the enhancement effect of aperiodic resonance, the spectral amplification factor is introduced as the evaluation index [35]. The index of spectral amplification factor η is defined as

$$\eta = \frac{\int_{f_{\min}}^{f_{\max}} X(f)df}{\int_{f_{\min}}^{f_{\max}} S(f)df}, \tag{10}$$

where $f_{\min}$ and $f_{\max}$ are the minimum instantaneous frequency and maximum instantaneous frequency of the NLFM signal, respectively. The functions $S(f)$ and $X(f)$ represent the amplitude of the spectrum of the original signal and system output, respectively.

3. Several kinds of typical NLFM signal

In this section, several kinds of NLFM signal are constructed to verify the validation of the piecewise re-scaled aperiodic resonance method.

3.1. The NLFM signal with increasing frequency over time

We take the signal in Eq. (2) as an example of NLFM signal with increasing frequency over time. Fig. 1 shows the time domain waveform, the amplitude spectrum and the short time Fourier transform (STFT) spectrum of the raw signal, respectively. The STFT spectrum is another good technique in modulated signal analysis. From these curves, we can see the difference of the NLFM signal from the harmonic signal and LFM signal.

Corresponding to the signal in Figs. 1,2 illustrates the spectral amplification factor η versus the system parameter b_1. The spectral amplification factor η at first increases with increasing the value of b_1, then reaches a maximum and falls again. This means that a resonance occurs in this case. Namely, the aperiodic resonance still can appear when the input signal in the nonlinear system is merely considered. It is evident that a strong resonance can be induced by an external signal only without the aid of noise (in SR) or another auxiliary signal (in VR). Moreover, the optimum system parameters for inducing aperiodic resonance can be determined by describing the resonance curve.

At the resonance peak in Fig. 2, *i.e.*, corresponding to the optimal system parameters, the optimal system output is obtained in Fig. 3. Compared with Figs. 1(a)–(b), Figs. 3 (a)–(b) show that the NLFM signal is effectively enhanced in the output. Meanwhile, by comparing Figs. 1(c) and 3(c), we find that the proposed method also extracts the time-varying characteristic frequency successfully. These results illustrate that the proposed method is effective in NLFM signal enhancement.

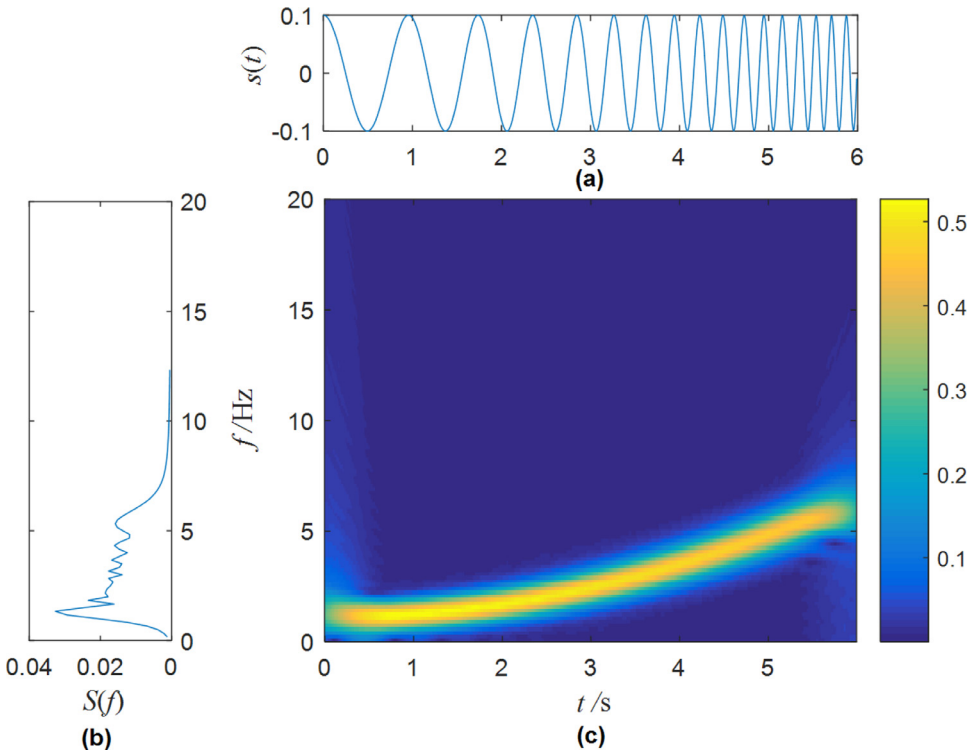

Fig. 1. The input NLFM signal, (a) the time domain waveform, (b) the amplitude spectrum, (c) the STFT spectrum. The simulation parameters are $A = 0.1$, $\gamma = 0.1$, $f_0 = 1$, $\varphi = 0$, $f_{\min} = 1$ and $f_{\max} = 6.4$.

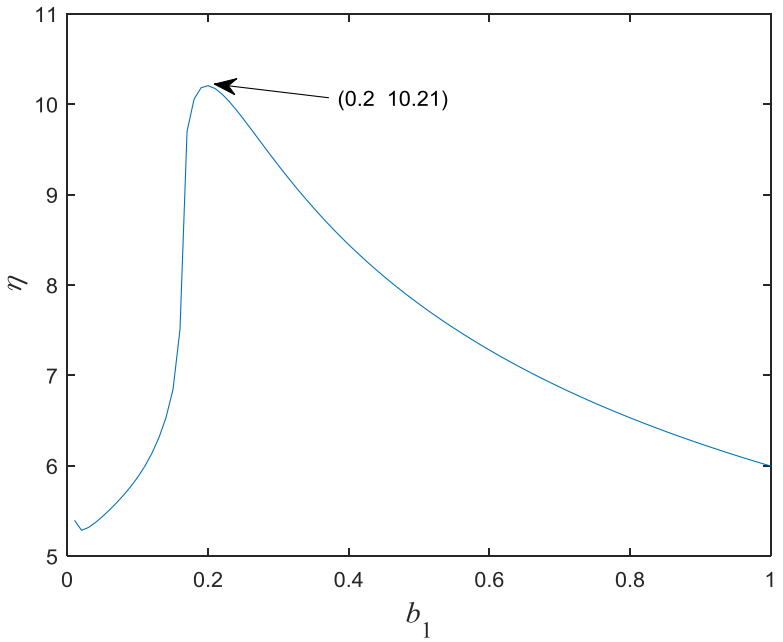

Fig. 2. The spectral amplification factor η versus the system parameter b_1. The simulation parameters are $a_1 = 0.01$, $\delta_1 = 0.2$, $m_0 = 1500$ and $d = 24$.

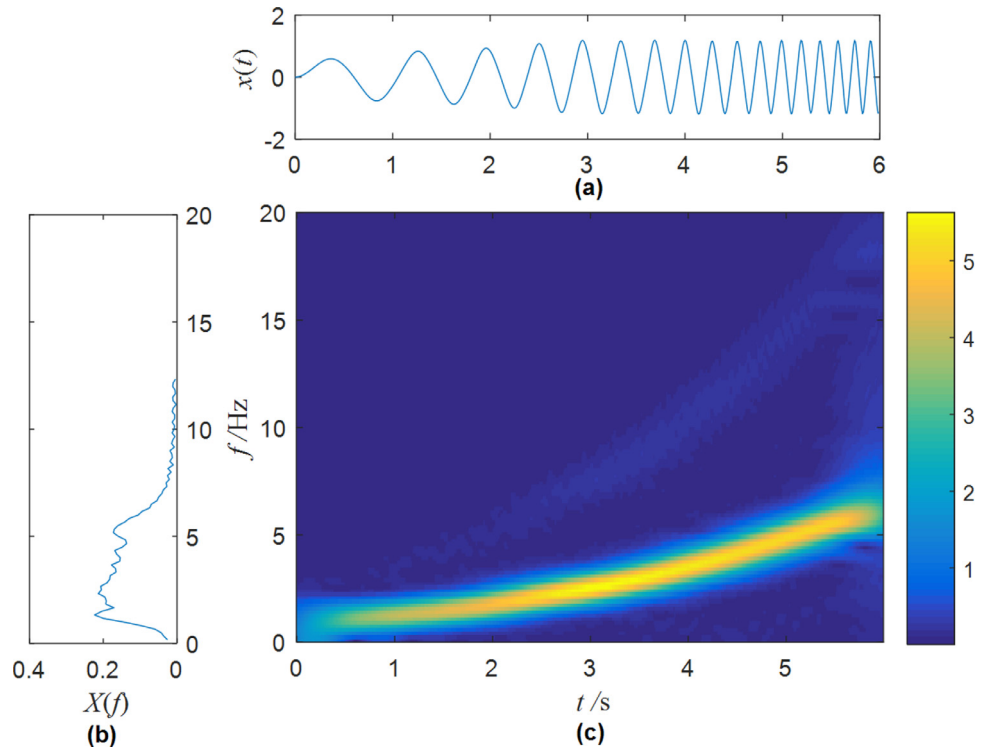

Fig. 3. The system output, (a) the time domain waveform, (b) the amplitude spectrum, (c) the STFT spectrum. The simulation parameters are $a_1 = 0.01$, $b_1 = 0.2$, $\delta_1 = 0.2$, $m_0 = 1500$ and $d = 24$.

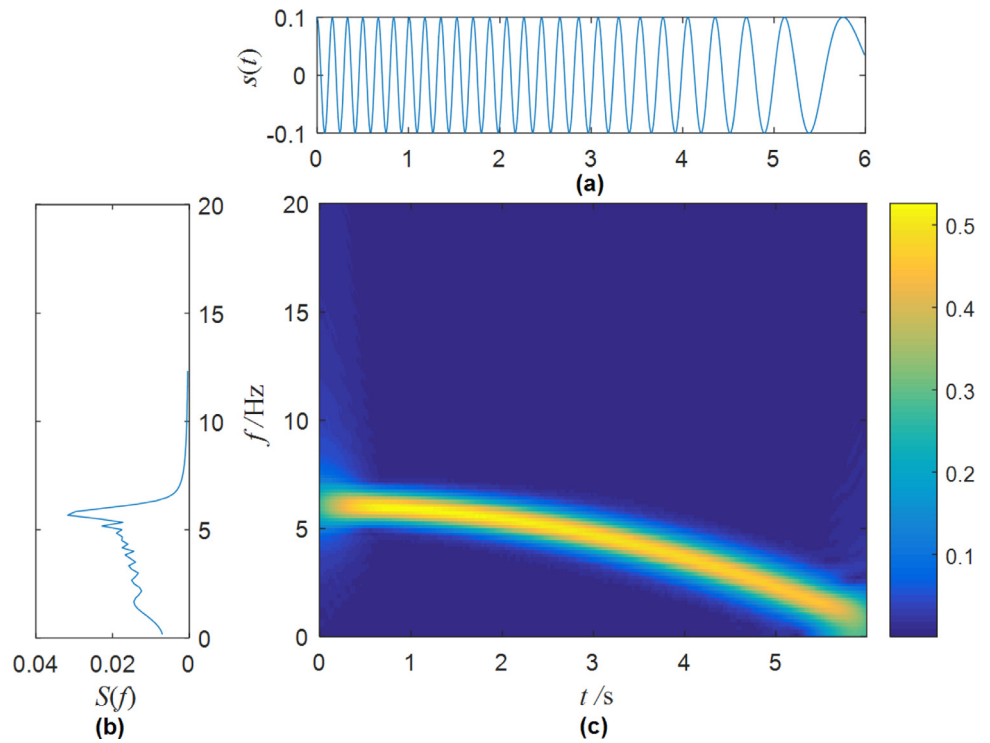

Fig. 4. The input NLFM signal, (a) the time domain waveform, (b) the amplitude spectrum, (c) the STFT spectrum. The simulation parameters are $A = 0.1$, $\gamma = 0.1$, $f_0 = 6$, $\varphi = 0$, $f_{\min} = 0.6$ and $f_{\max} = 6$.

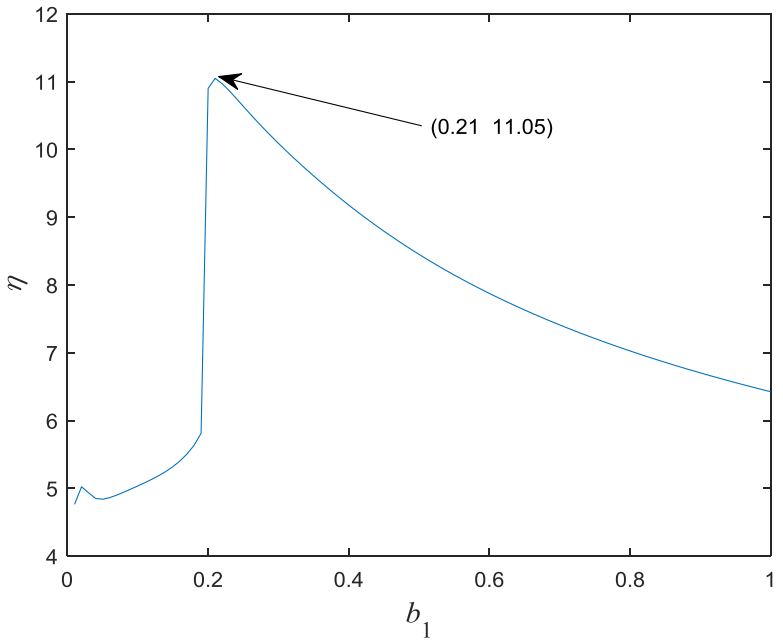

Fig. 5. The spectral amplification factor η versus the system parameter b_1. The simulation parameters are $a_1 = 0.01$, $\delta_1 = 0.2$, $m_0 = 1500$ and $d = 24$.

3.2. The NLFM signal with decreasing frequency over time

With the increase of time, the NLFM signal with decreasing frequency is as follow

$$s(t) = s_2(t) = A\cos\left(-\pi\gamma t^3 + 2\pi f_0 t + \varphi\right) \tag{11}$$

Fig. 4 shows the time domain waveform, the amplitude spectrum and the STFT spectrum of the NLFM signal in Eq. (11). Fig. 5 describes the spectral amplification factor η versus the system parameter b_1. With the increase of the system parameter b_1, the spectral amplification factor η increases first and then decreases. The peak value appears in the resonance curve. It shows that the resonance still occurs under appropriate system parameters, even there is only a single external signal in the excitation. Compared with Fig. 2, the curve in Fig. 5 represents the same trend. Under the optimal system parameters, the aperiodic resonance output is obtained as shown in Fig. 6. By comparing Figs. 4(a)–(b) with Figs. 6(a)–(b), we find that the NLFM signal is enhanced successfully. Meanwhile, comparing with Fig. 4(c), Fig. 6(c) illustrates that the proposed method also extracts the time-varying characteristic frequency. Thus, the NLFM signal can be enhanced based on the proposed method.

3.3. The NLFM signal with frequency first increasing and then fixed over time

The frequency of the NLFM signal increases first and then remains unchanged over time. The NLFM signal is as follows

$$s(t) = s_3(t) = \begin{cases} A\cos\left(\pi\gamma t^3 + 2\pi f_0 t + \varphi\right) & 0 \le t \le t_1 \\ A\cos\left[\left(3\pi\gamma t_1^2 + 2\pi f_0\right)t + \varphi\right] & t_1 < t \end{cases}, \tag{12}$$

where t_1 is the critical time of frequency conversion.

Figs. 7(a)–(c) corresponds to the time domain waveform, the amplitude spectrum and the STFT spectrum of $s(t)$ in Eq. (12), respectively. Fig. 8 represents the spectral amplification factor η versus the system parameter b_1. Firstly, the spectral amplification factor η increases with the increasing of system parameter b_1, but then reaches the maximum and decreases again. Compared with the previous resonance curve, the curve in Fig. 8 shows the same trend. Namely, when the input signal of the nonlinear system is only considered, the aperiodic resonance phenomenon still occurs. The system output in Fig. 9 is obtained through the optimal parameters. Compared with the raw NLFM signal in Fig. 7, the enhancement of the NLFM signal is illustrated in Figs. 9(a)–(b) and the time-varying characteristic frequency is extracted in Fig. 9(c). These similar results show that the proposed method can be used to enhance the NLFM signal.

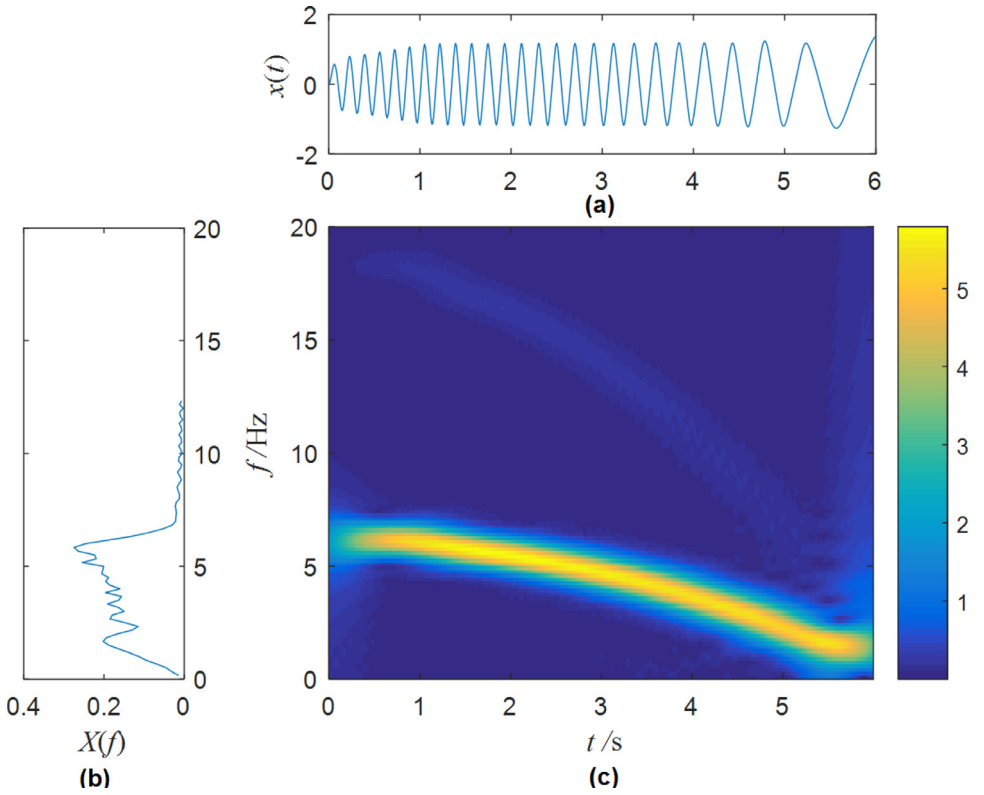

Fig. 6. The system output, (a) the time domain waveform, (b) the amplitude spectrum, (c) the STFT spectrum. The simulation parameters are $a_1 = 0.01$, $b_1 = 0.21$, $\delta_1 = 0.2$, $m_0 = 1500$ and $d = 24$.

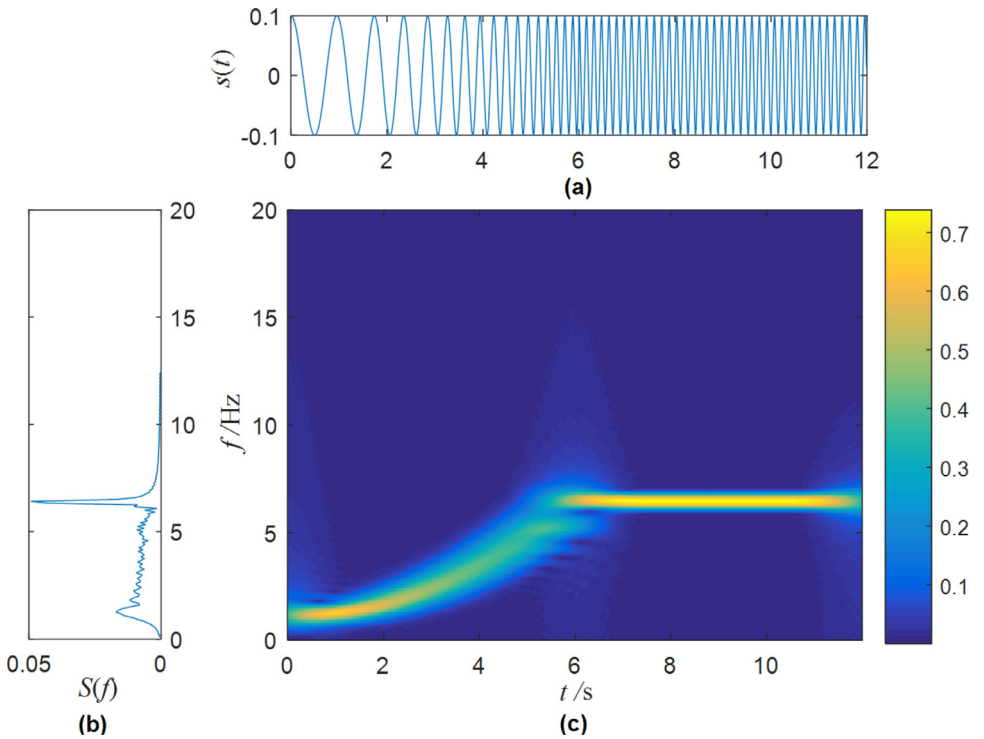

Fig. 7. The input NLFM signal, (a) the time domain waveform, (b) the amplitude spectrum, (c) the STFT spectrum. The simulation parameters are $A = 0.1$, $\gamma = 0.1$, $f_0 = 1$, t_1=6, $\varphi = 0$, $f_{\min} = 1$ and $f_{\max} = 6.4$.

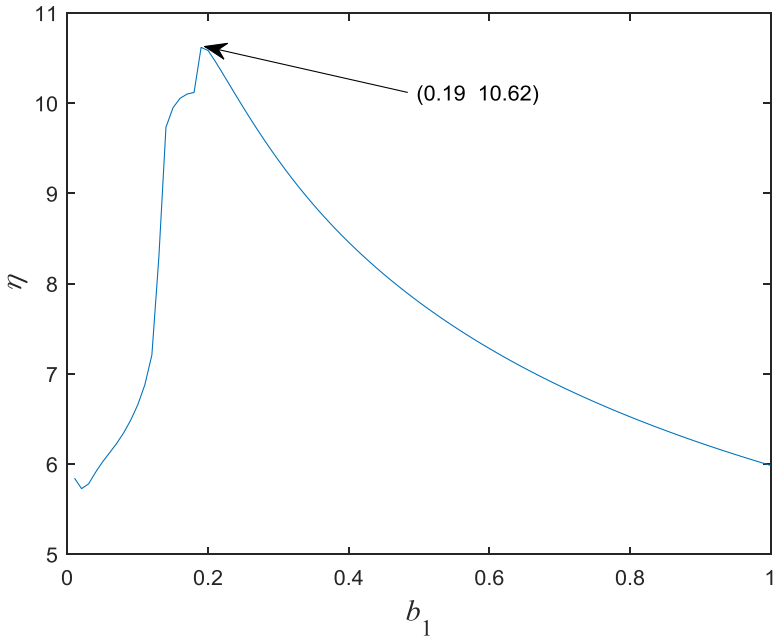

Fig. 8. The spectral amplification factor η versus the system parameter b_1. The simulation parameters are $a_1 = 0.01$, $\delta_1 = 0.2$, $m_0 = 1500$ and $d = 24$.

3.4. The NLFM signal with frequency first invariant and then decreased over time

With the increase of time, the NLFM signal whose frequency remains unchanged and then decreases is as follows

$$s(t) = s_4(t) = \begin{cases} A\cos\left(2\pi f_0 t + \varphi\right) & 0 \le t \le t_1 \\ A\cos\left[-\pi\gamma\left(t - t_1\right)^3 + 2\pi f_0(t - t_1) + \varphi\right] & t_1 < t \end{cases} \tag{13}$$

where t_1 is the critical time of frequency conversion.

Fig. 10 gives the time domain waveform, the amplitude spectrum and the STFT spectrum of $s(t)$ in Eq. (13). Fig. 11 represents the spectral amplification factor η versus the system parameter b_1. The maximum value of the spectral amplification factor η is appeared with increasing of system parameter b_1. Once again, they show aperiodic resonance without any auxiliary signal or noise. Meanwhile, the results show that the system parameters is a key factor to induce aperiodic resonance. Thus, the resonance curve in Fig. 11 is used to determine the optimal system parameters. Under the optimal system parameters, the system output is obtained as shown in Fig. 12. Comparing the input NLFM signal in Figs. 10(a)-(b) with the system output in Figs. 12(a)–(b), we find that the NLFM signal is enhanced successfully. Moreover, the time-varying characteristic frequency is also extracted in Fig. 12(c). Compared with the previous results, Figs. 10–12 further illustrates the effectiveness of the proposed method.

3.5. The NLFM signal with frequency first increased and then invariant and final decreased over time

In this subsection, the studied NLFM signal is as follows

$$s(t) = s_5(t) = \begin{cases} A\cos\left(\pi\gamma t^3 + 2\pi f_0 t + \varphi\right) & 0 \le t \le t_1 \\ A\cos\left[\left(3\pi\gamma {t_1}^2 + 2\pi f_0\right)t + \varphi\right] & t_1 < t \le t_2 \\ A\cos\left[-\pi\gamma\left(t - t_2\right)^3 + \left(3\pi\gamma {t_1}^2 + 2\pi f\right) \times (t - t_2) + \varphi\right] & t_2 < t \end{cases} \tag{14}$$

where t_1, t_2 are the critical time of frequency conversion.

Figs. 13(a)–(c) corresponds to the time domain waveform, the amplitude spectrum and the STFT spectrum of $s(t)$ in Eq. (14), respectively. Fig. 14 illustrates the spectral amplification factor η versus the system parameter b_1. The peak value in the curve means that the aperiodic resonance appears. The result shows that aperiodic resonance can be induced by tuning system parameters even without auxiliary signal or noise. Fig. 15 shows the system output under the optimal system parameters. Through the analysis of Figs. 13(a)–(b) and Figs. 15(a)–(b), the NLFM signal is enhanced by the proposed method. Moreover, in Fig. 15(c), this method also extracts the time-varying characteristic frequency. This indicates that the proposed method can enhance the NLFM signal effectively once again.

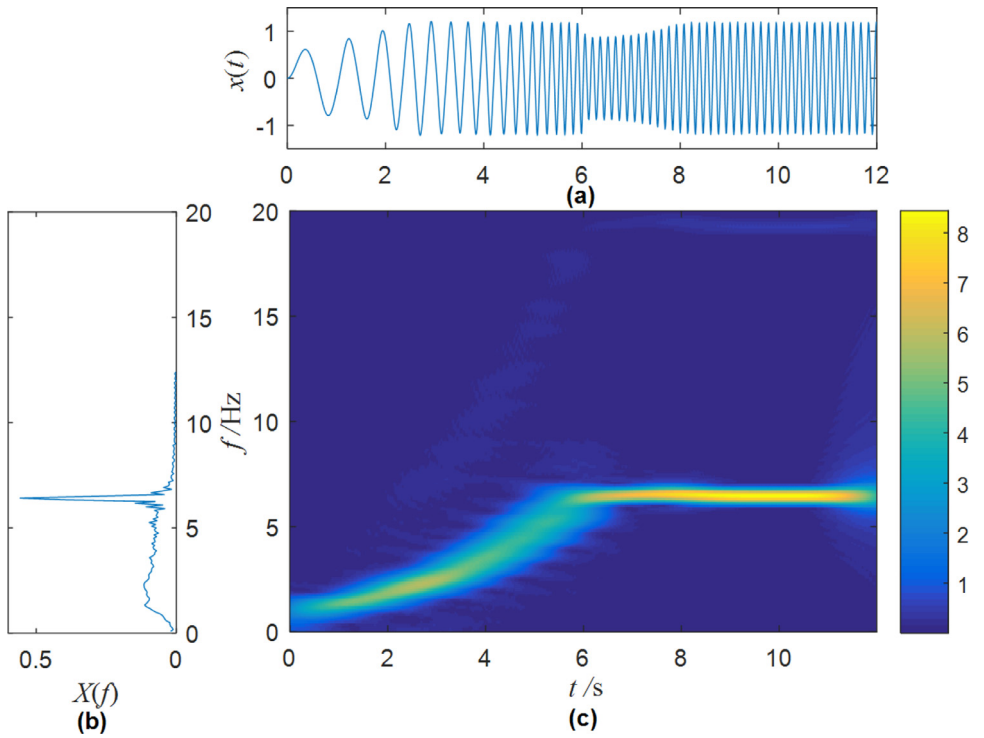

Fig. 9. The system output, (a) the time domain waveform, (b) the amplitude spectrum, (c) the STFT spectrum. The simulation parameters are $a_1 = 0.01$, $b_1 = 0.19$, $\delta_1 = 0.2$, $m_0 = 1500$ and $d = 24$.

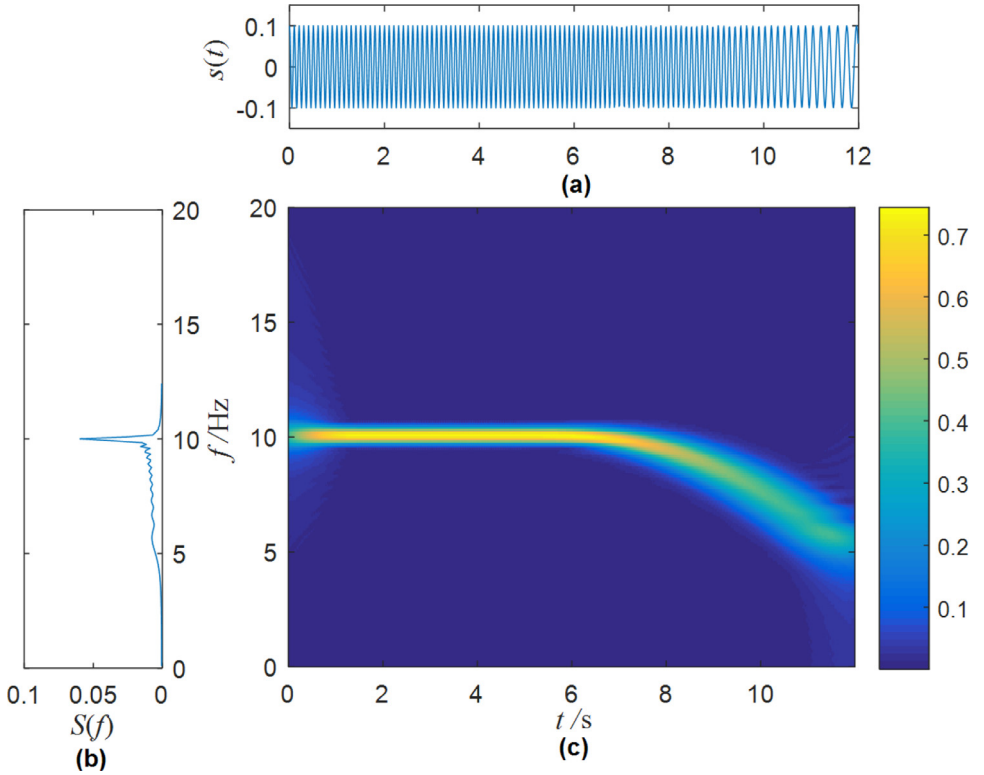

Fig. 10. The input NLFM signal, (a) the time domain waveform, (b) the amplitude spectrum, (c) the STFT spectrum. The simulation parameters are $A = 0.1$, $\gamma = 0.1$, $f_0 = 10$, $t_1 = 6$, $\varphi = 0$, $f_{\min} = 4.6$ and $f_{\max} = 10$.

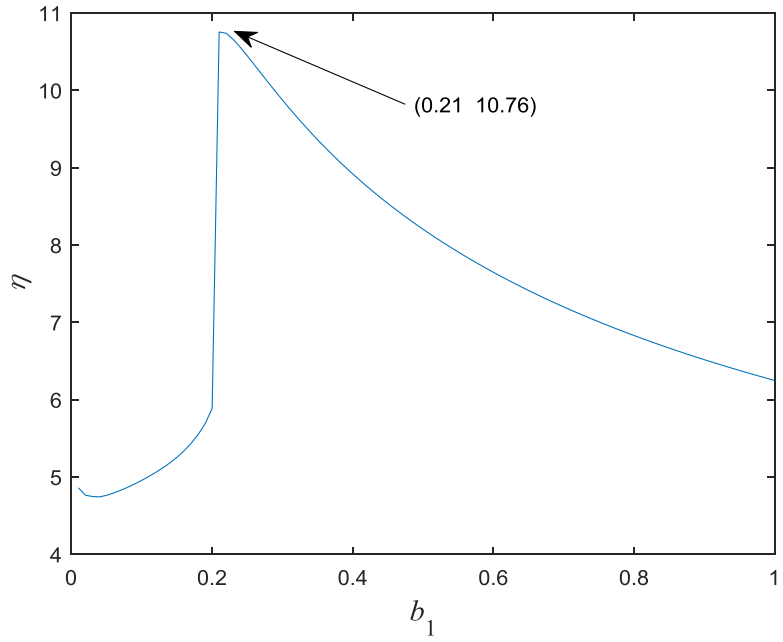

Fig. 11. The spectral amplification factor η versus the system parameter b_1. The simulation parameters are $a_1 = 0.01$, $\delta_1 = 0.2$, $m_0 = 1500$ and $d = 24$.

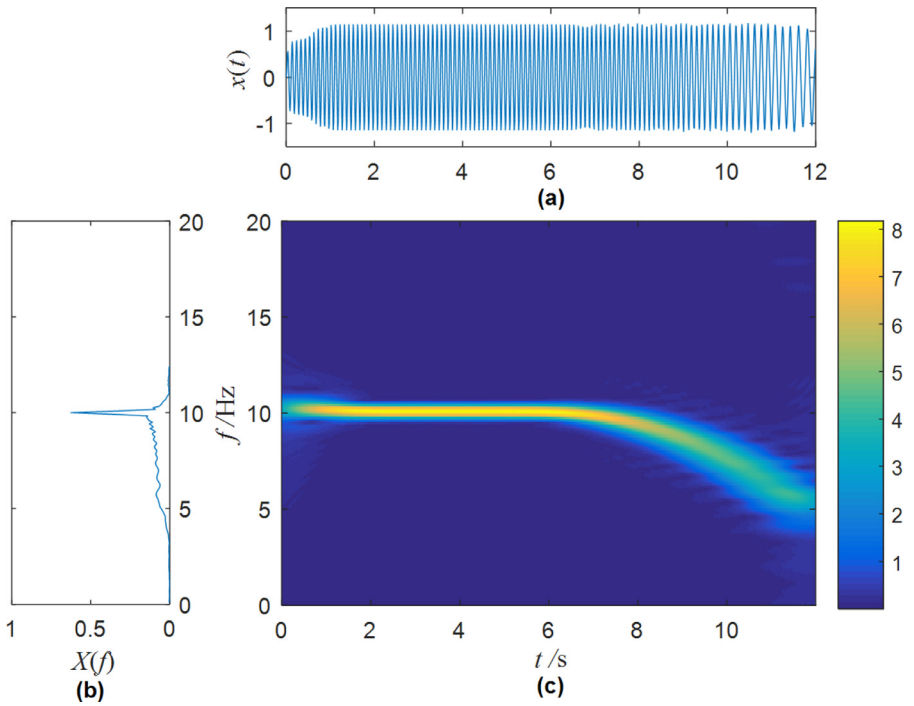

Fig. 12. The system output, (a) the time domain waveform, (b) the amplitude spectrum, (c) the STFT spectrum. The simulation parameters are $a_1 = 0.01$, $b_1 = 0.21$, $\delta_1 = 0.2$, $m_0 = 1500$ and $d = 24$.

3.6. The NLFM signal with noise

In this subsection, we use the method to process the NLFM signal with noise. In strong background noise, the signal processing method is different from the proposed method in this manuscript [41]. Hence, the noise is not very strong here. As mentioned in the Introduction section, the research in this paper is different from the signal enhancement methods of SR and VR. The resonance phenomenon is realized without the aid of additional noise or auxiliary signal. To study aperiodic

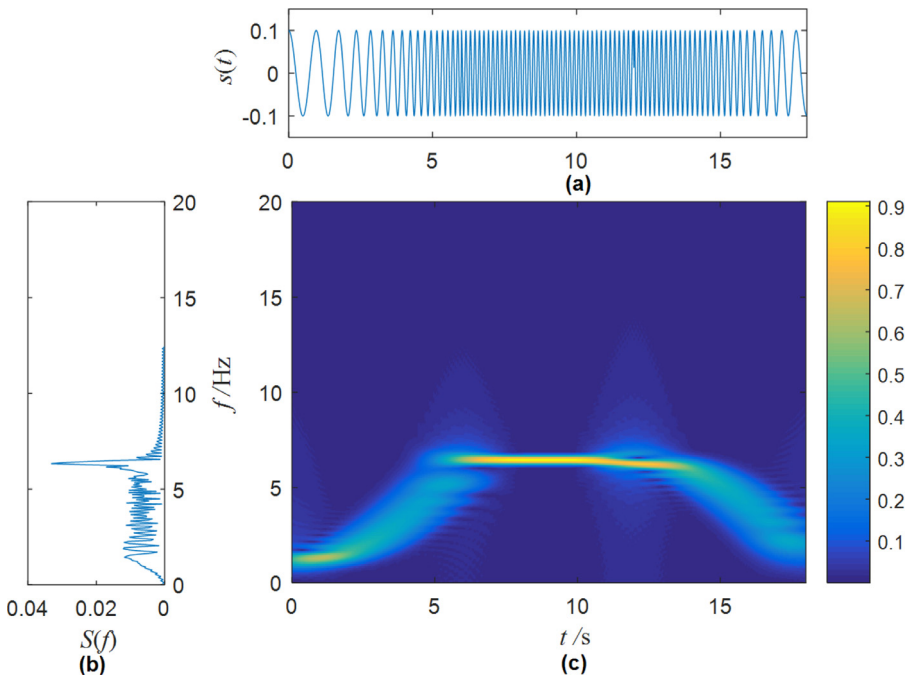

Fig. 13. The input NLFM signal, (a) the time domain waveform, (b) the amplitude spectrum, (c) the STFT spectrum. The simulation parameters are $A = 0.1$, $\gamma = 0.1$, $f_0 = 1$, $t_1 = 6$, $t_2 = 12$, $\varphi = 0$, $f_{\min} = 1$ and $f_{\max} = 6.4$.

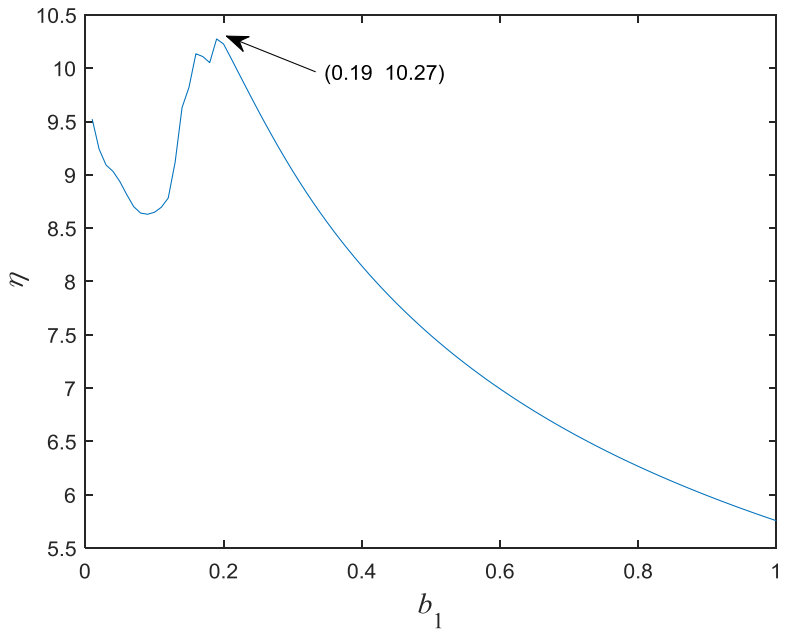

Fig. 14. The spectral amplification factor η versus the system parameter b_1. The simulation parameters are $a_1 = 0.01$, $\delta_1 = 0.2$, $m_0 = 1500$ and $d = 36$.

resonance for processing the NLFM signal with noise, we add Gaussian white noise $\xi(t)$ to the NLFM signal $s_1(t)$. Here, the statistical property of the Gaussian white noise is

$$\langle \xi(t) \rangle = 0, \ \left\langle \xi(t)\xi\left(t'\right) \right\rangle = 2D\delta(t - t') \tag{15}$$

Fig. 16 shows the NLFM signal $s_1(t)$ with noise intensity $D = 0.01$. The signal is obviously polluted by the noise. Fig. 17 illustrates the spectral amplification factor η versus the system parameter b_1. The peak value in the curve indicates that the aperiodic resonance appears. Meanwhile, the curve also give an optimal b_1 to induce aperiodic resonance. Next, based on the optimal system parameter, we get Fig. 18 by using the proposed method. Comparing the STFT spectrum of Fig. 16 and

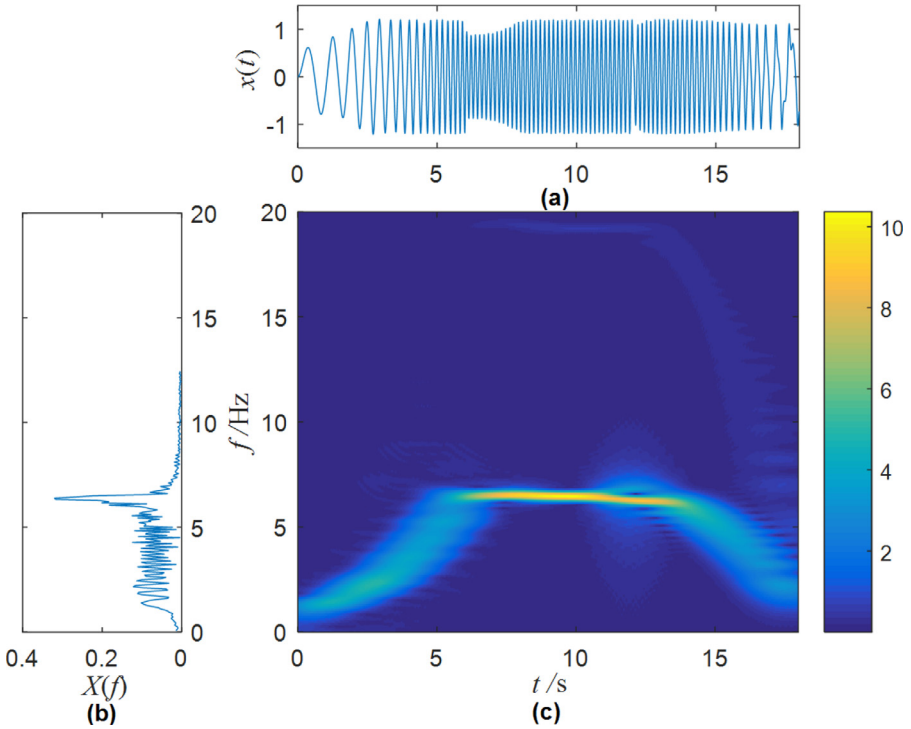

Fig. 15. The system output, (a) the time domain waveform, (b) the amplitude spectrum, (c) the STFT spectrum. The simulation parameters are $a_1 = 0.01$, $b_1 = 0.2$, $\delta_1 = 0.2$, $m_0 = 1500$ and $d = 36$.

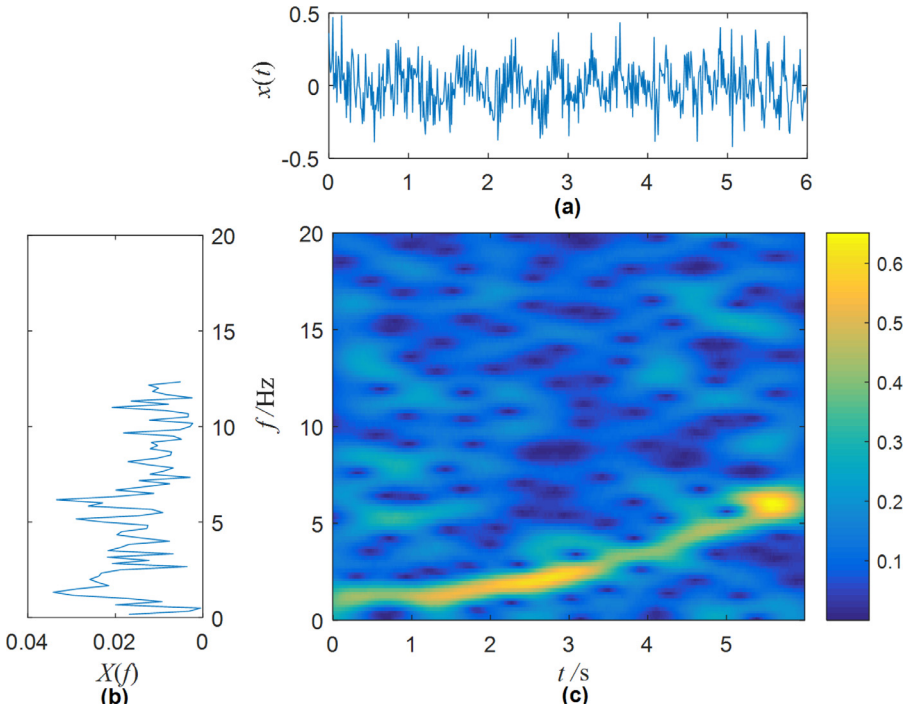

Fig. 16. The input NLFM signal with weak noise, (a) the time domain waveform, (b) the amplitude spectrum, (c) the STFT spectrum. The simulation parameters are $A = 0.1$, $\gamma = 0.1$, $f_0 = 1$, $\varphi = 0$, $D = 0.01$, $f_{\min} = 1$ and $f_{\max} = 6.4$.

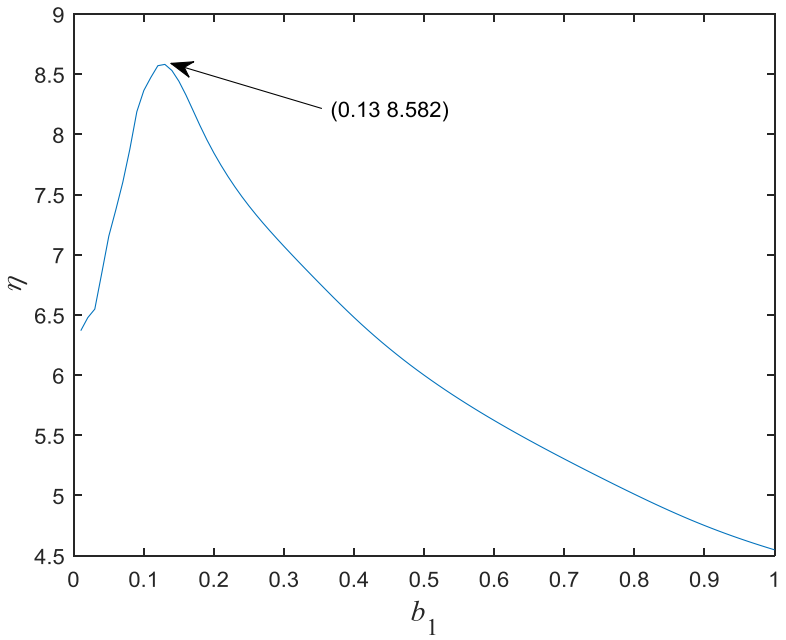

Fig. 17. The spectral amplification factor η versus the system parameter b_1. The simulation parameters are $a_1 = 0.01$, $\delta_1 = 0.2$, $m_0 = 1500$ and $d = 24$.

Fig. 18, we can observe that the NLFM signal with noise is enhanced effectively. In addition, we also find that the noise is removed. It illustrates that the aperiodic resonance still represents a favorable performance for processing the NLFM signal with noise.

4. Experimental verification

In order to extend the application of the proposed method, we use the experimental signal to verify the feasibility of this method. The experimental signal is a bearing fault vibration signal with time-varying characteristic frequency, which is obtained under variable speed condition.

4.1. The experimental rig

The experimental signal is collected from the experimental rig, as shown in Fig. 19. First, acceleration senor with type 1A206E collects the vibration signal. Then, the vibration signal is transmitted to laptop by acquisition card with type NI9234. Finally, by using the LabVIEW software and DAQmx driver, the experimental signal is read. In addition, frequency converter controls the speed of motor with type 198 BGL-H 5P5 15/80 to meet the requirement of variable speed. Meanwhile, torque sensor and radial loading device provide the brake torque and the radial force, respectively. The types of them are JN-DN and ZQ-21B-1.

The training bearing with type N306E is used in the test, which has a scratch in the outer ring. The specific size of the scratch is 0.5 mm × 1.2 mm (depth × width). The theoretical fault frequency f_o of the bearing outer ring is

$$f_o = \frac{ZN}{120}\left(1 - \frac{D_r}{D_p}\cos\alpha\right) \tag{16}$$

In this section, the number of rolling elements $Z = 11$, the diameter of rolling element $D_r = 10$ mm, the pitch diameter of the bearing $D_p = 52$ mm, the contact angle $\alpha = 0$. The rotational speed N in this test increases from 10 Hz to 25 Hz. According to Eq. (16), f_o increases from 44.423 Hz to 111.056 Hz.

4.2. The processing of the experimental signal

Fig. 20 gives the time domain waveform, the amplitude spectrum and the STFT spectrum of the experimental signal. In the STFT spectrum, we get the time-varying characteristic frequency of bearing fault and its superharmonic component. Fig. 21 represents the aperiodic resonance directly excited by the aperiodic signal. The value of b_1 at the peak of curve is the optimal system parameter for induced aperiodic resonance. Subsequent, under the optimal system parameter, we obtain Fig. 22 by the proposed method. In Fig. 22(c), the time-varying characteristic frequency of bearing fault is enhanced by this method. Meanwhile, it also extracts the time-varying characteristic frequency of bearing fault. In addition, its interference

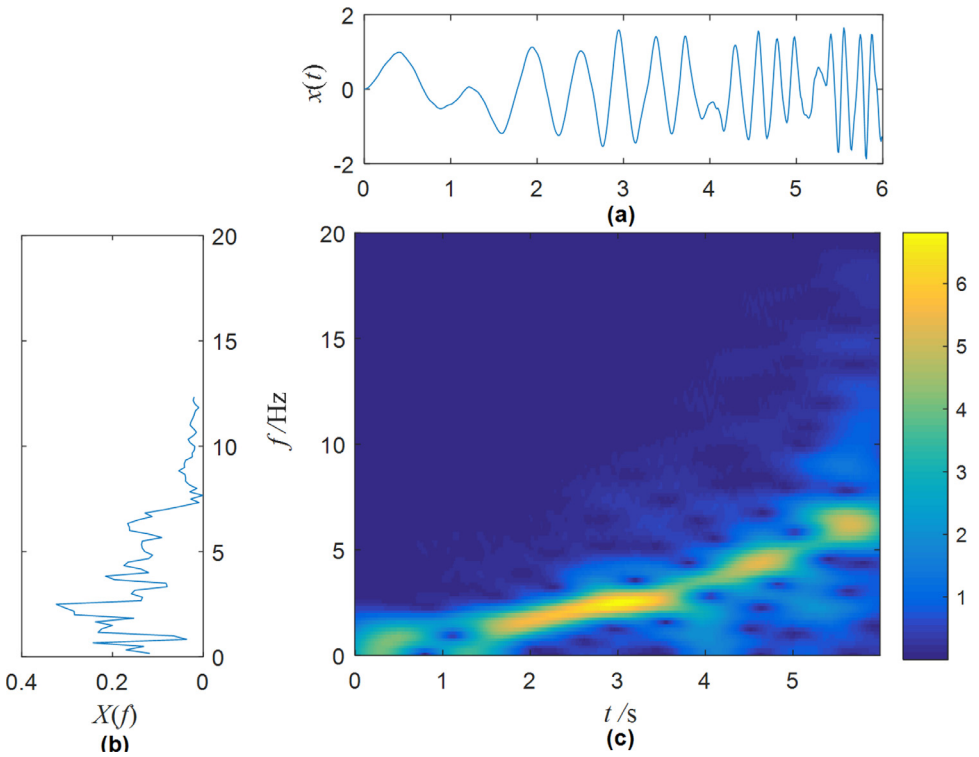

Fig. 18. The system output, (a) the time domain waveform, (b) the amplitude spectrum, (c) the STFT spectrum. The simulation parameters are $a_1 = 0.01$, $b_1 = 0.13$, $\delta_1 = 0.2$ $m_0 = 1500$, and $d = 24$.

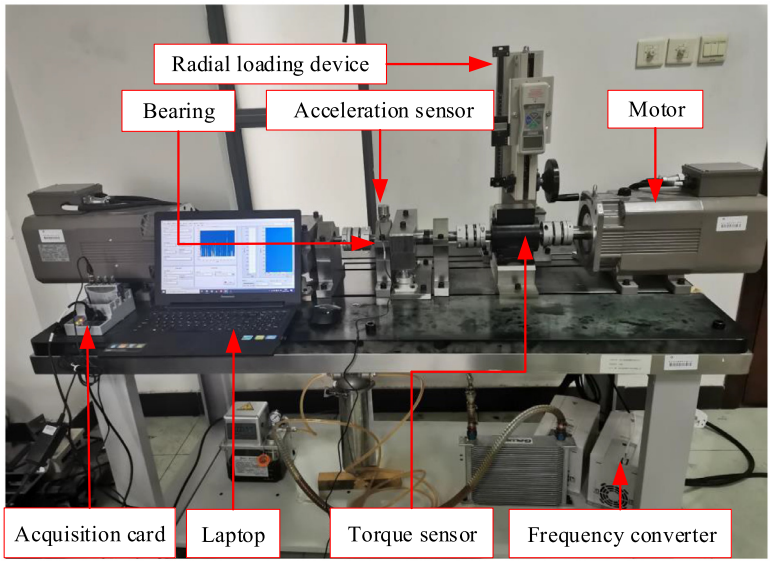

Fig. 19. The experimental rig.

superharmonic components are almost removed. The results show that the re-scaled aperiodic resonance method is also effective in bearing fault diagnosis.

A Gaussian white noise is added to the experimental signal to simulate the noise background. The experiment signal with noise $D = 300$ is shown in Fig. 23. Here, we must emphasized that unit of the vibration signal is *mV*. The amplitude of the vibration signal is large in this unit. Hence, the noise intensity is also large here. The curve in Fig. 24 shows that the aperiodic resonance is excited by this signal. By using the proposed method, we get Fig. 25. It illustrates that the time-varying characteristic frequency of bearing fault is enhanced. Meanwhile, the noise and other interference superharmonic

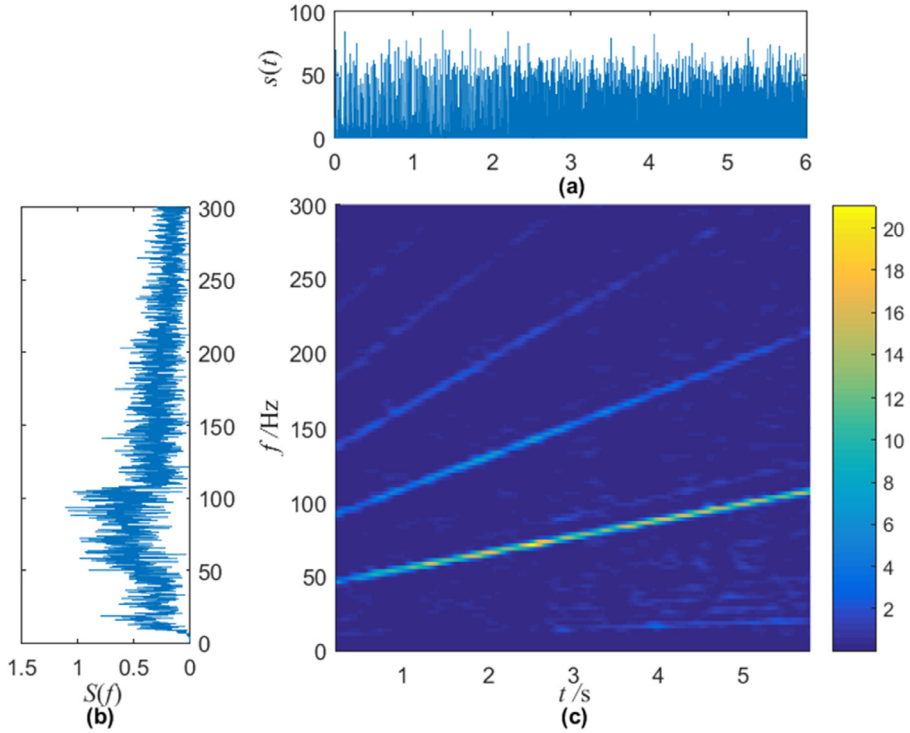

Fig. 20. The input experimental signal, (a) the time domain waveform, (b) the amplitude spectrum, (c) the STFT spectrum. The parameters are $f_{\min} = 44.423$ Hz and $f_{\max} = 111.056$ Hz.

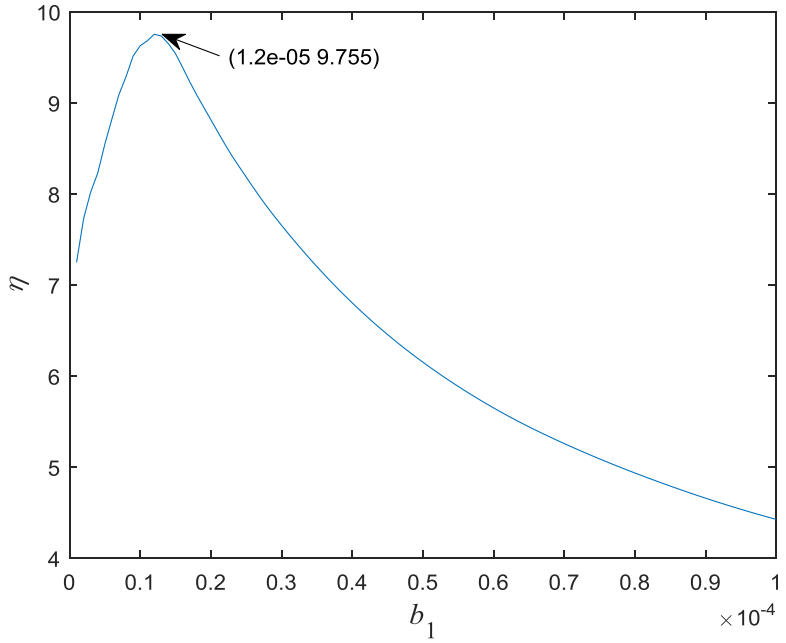

Fig. 21. The spectral amplification factor η versus the system parameter b_1. The simulation parameters are $a_1 = 0.01$, $\delta_1 = 0.2$, $m_0 = 1500$ and $d = 40$.

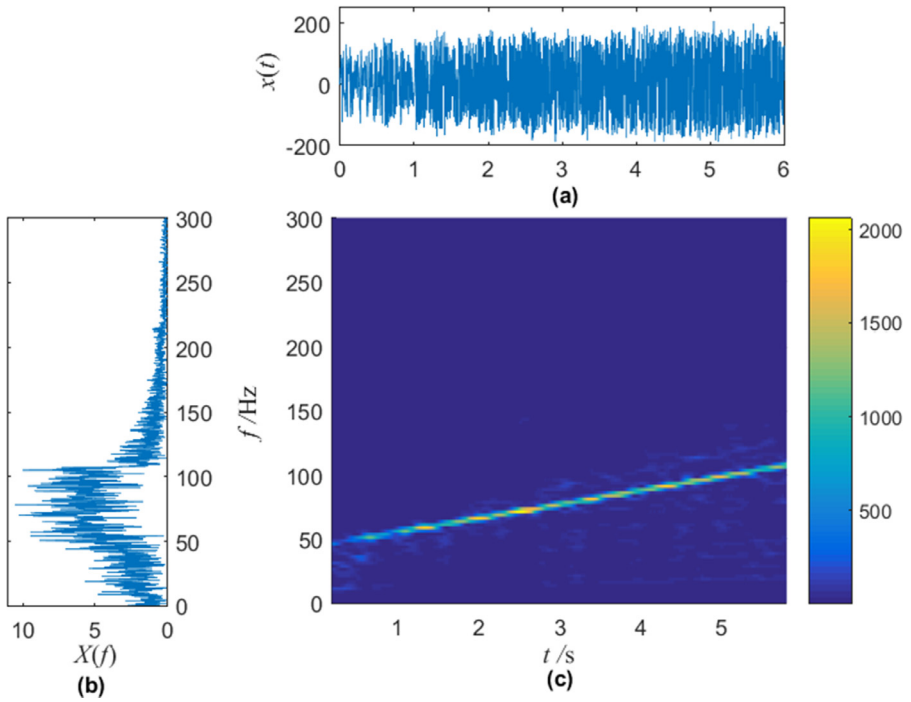

Fig. 22. The system output, (a) the time domain waveform, (b) the amplitude spectrum, (c) the STFT spectrum. The simulation parameters are $a_1 = 0.01$, $b_1 = 0.000012$, $\delta_1 = 0.2$, $m_0 = 1500$ and $d = 40$.

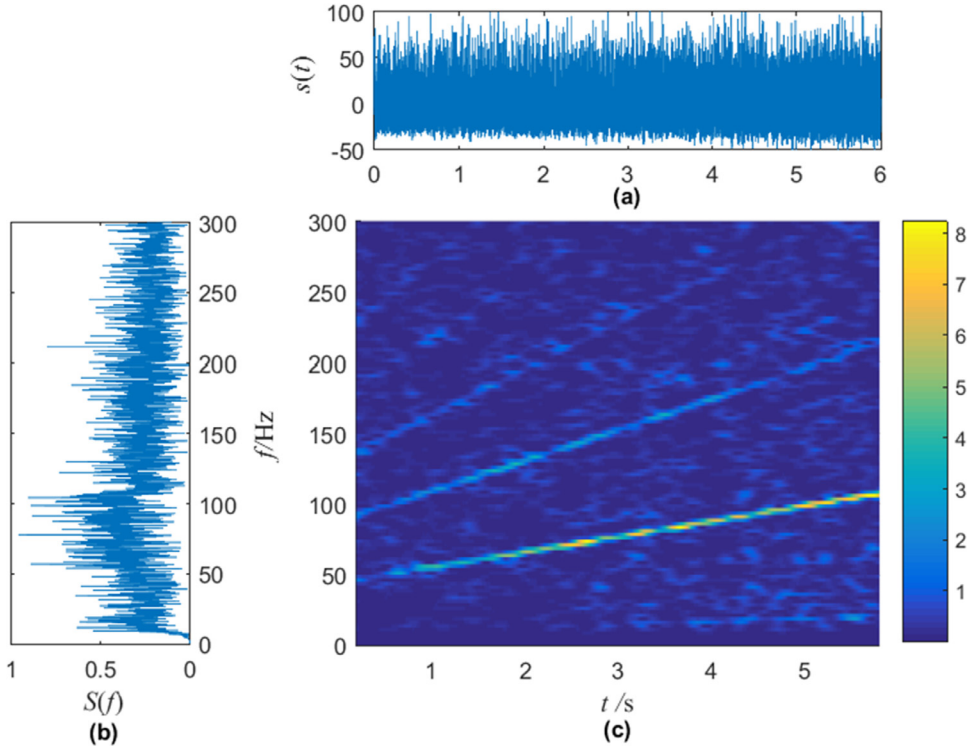

Fig. 23. The input experimental signal with noise, (a) the time domain waveform, (b) the amplitude spectrum, (c) the STFT spectrum. The parameters are $f_{\min} = 44.423$ Hz and $f_{\max} = 111.056$ Hz.

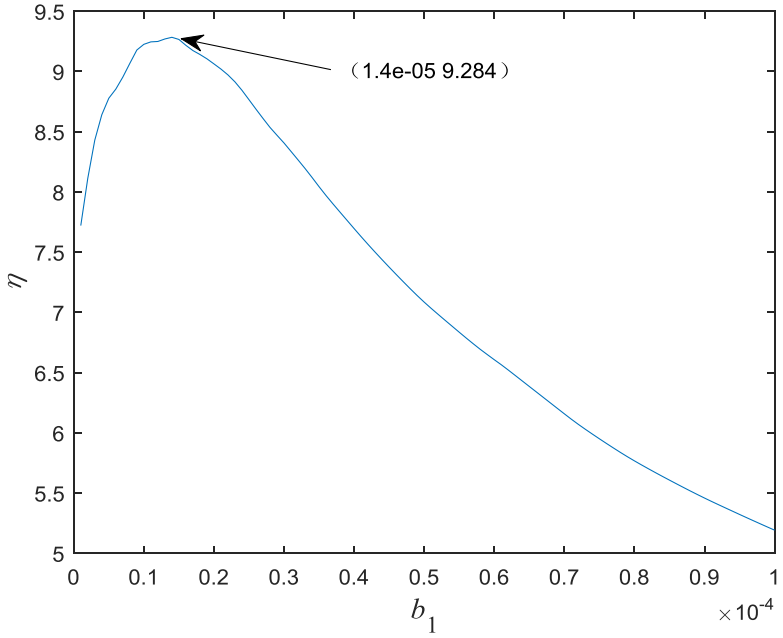

Fig. 24. The spectral amplification factor η versus the system parameter b_1. The simulation parameters are $a_1 = 0.01$, $\delta_1 = 0.2$, $m_0 = 1500$ and $d = 40$.

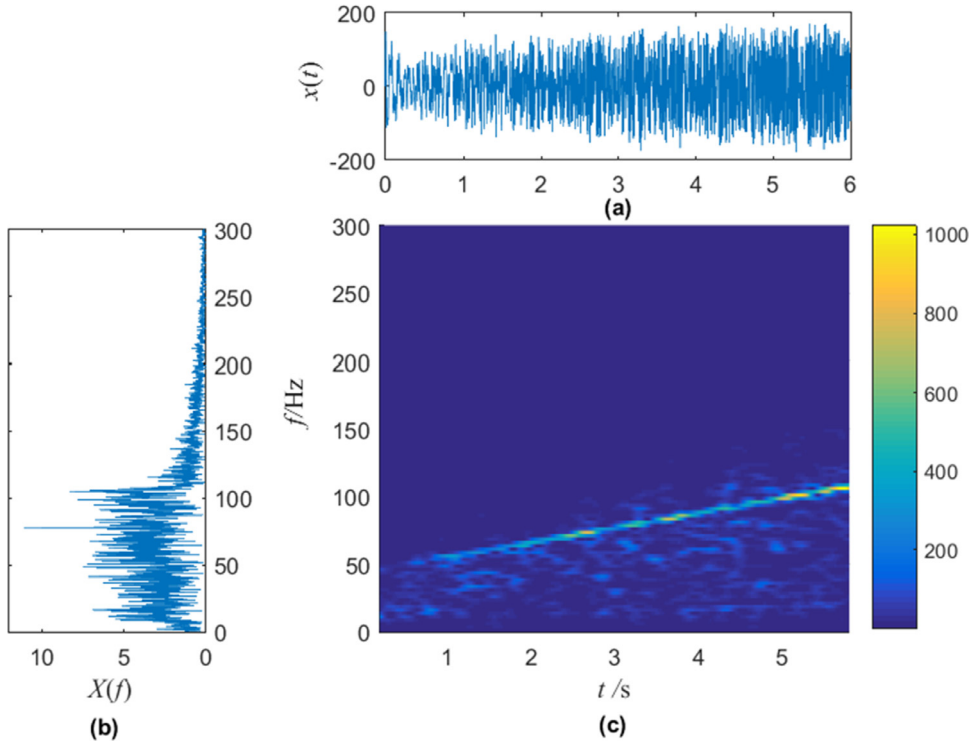

Fig. 25. The system output, (a) the time domain waveform, (b) the amplitude spectrum, (c) the STFT spectrum. The simulation parameters are $a_1 = 0.01$, $b_1 = 0.000014$, $\delta_1 = 0.2$, $m_0 = 1500$ and $d = 40$.

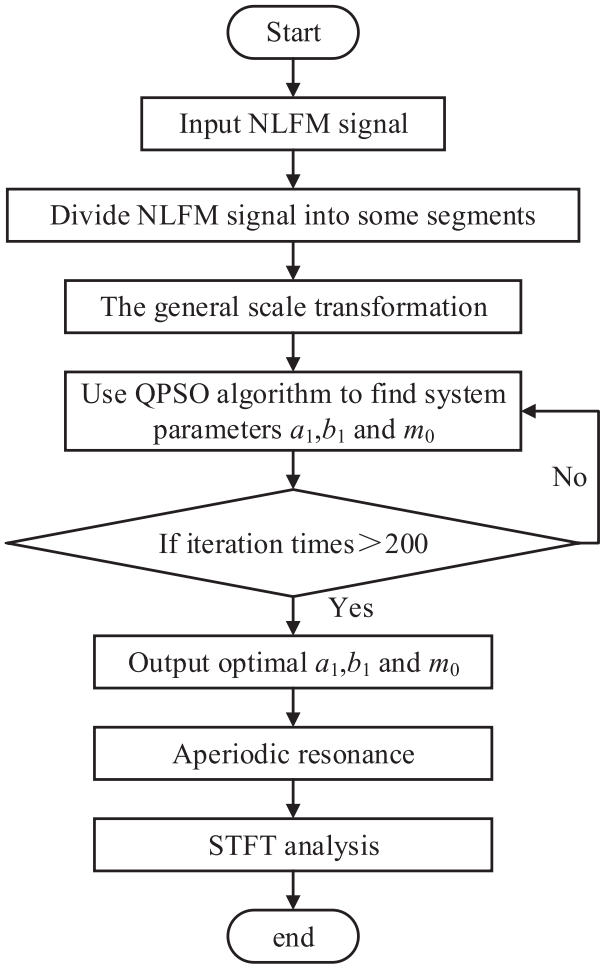

Fig. 26. The flow chart of the adaptive piecewise re-scaled aperiodic resonance method.

components are almost removed. In a word, the results show that the proposed method has an excellent effect even in noise background.

5. Adaptive piecewise re-scaled aperiodic resonance method

In the previous sections, the optimal parameters of aperiodic resonance are determined by characterizing the resonance curve. In the process of finding the optimal parameters, on the one hand, it is unnecessary to make an iteration loop to find the peak value of the resonance curve. On the other hand, the precision of the result depends on the step setting in the iteration loop. Thus, this process is complicated and takes a long time, which may have a negative role on the application of the proposed method. In order to solve this problem, an optimization algorithm is introduced in this paper. Based on the optimization algorithm, the system parameters are adaptively selected to simplify the processing flow and improve the computational efficiency of the method.

Here, the spectrum amplification factor is used as the fitness function. Meanwhile, the quantum particle swarm optimization (QPSO) algorithm is used to quickly find the optimal parameters [42]. The algorithm steps are as follows,

(1) The maximum iteration times is set to 200. The number of particle swarm is set to 50, where each particle position represents a potential solution. Search space is set to $a_1 \in (0.01, 2)$, $b_1 \in (0.01, 2)$ and $m_0 \in (100, 5000)$.
(2) According to the fitness function, the fitness value of each particle is calculated at the initial position. Meanwhile, the fitness value obtained is taken as the elitist of the first generation of particles. The maximum value is regarded as the global optimal fitness value.
(3) Start the iteration. The position of the particle is adaptively updated in each iteration.
(4) Update the position of the particle and calculate the fitness value of each particle.

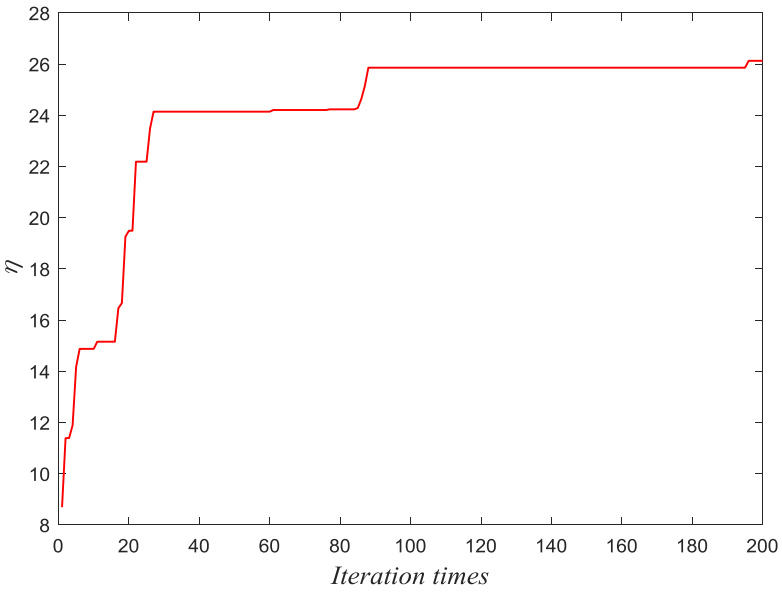

Fig. 27. Iterative process of the adaptive piecewise re-scaled aperiodic resonance method.

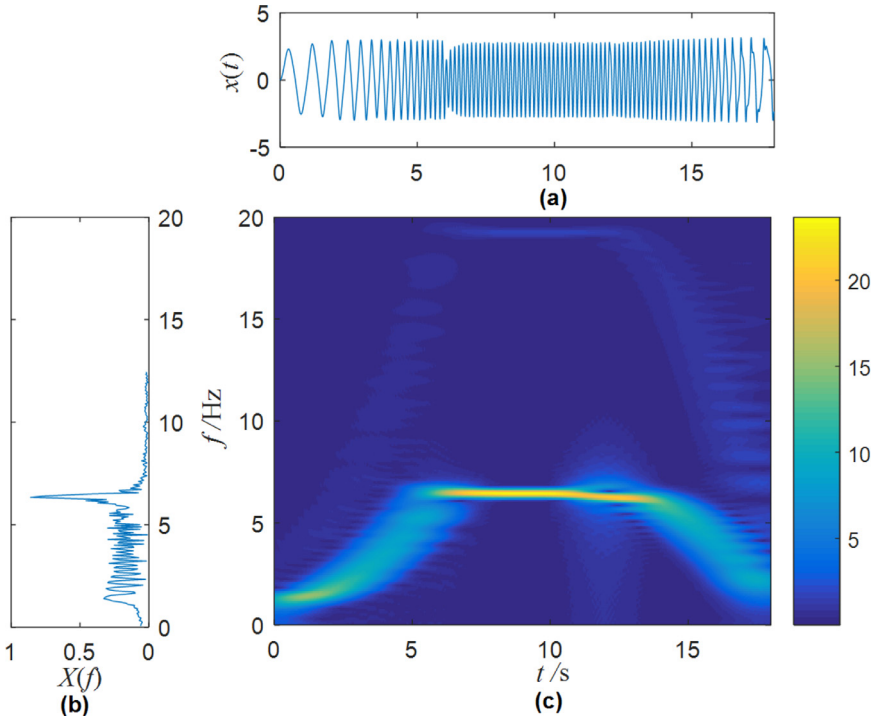

Fig. 28. The system output obtained by adaptive aperiodic resonance, (a) the time domain waveform, (b) the amplitude spectrum, (c) the STFT spectrum. The simulation parameters are $a_1 = 0.0269$, $b_1 = 0.012$, $\delta_1 = 0.2$, $m_0 = 3494$ and $d = 36$.

(5) The fitness value of the elitist is updated by comparing with the last iteration. At the same time, the elitist is compared with the global optimal fitness value. If it is better than the global optimization, it is regarded as a new global optimal fitness value.
(6) Repeat steps (3) to (5) until the number of iterations reaches 200.
(7) When the number of iterations reaches the maximum iteration times, the current optimal value is output.

Combined with the QPSO algorithm, the specific process of an adaptive piecewise re-scaled aperiodic resonance method is shown in Fig. 26. The NLFM signal in subSection 3.5 is taken as an example to verify the validation of the proposed method. Fig. 27 gives the convergence curve of the adaptive piecewise re-scaled aperiodic resonance method. The conver-

gence curve can converge quickly until the iteration times reaches 90. At this point, the optimal parameters are obtained by QPSO algorithm, which are $a_1 = 0.0269$, $b_1 = 0.012$, $m_0 = 3494$, respectively. Under the optimum parameters, the system output is obtained as shown in Fig. 28. The value of the spectrum amplification factor is much larger than the peak value in Fig. 14. It illustrate a much stronger resonance performance. It is because we search the optimal system parameters a_1 and b_1 simultaneously. In Fig. 14, only the optimal b_1 is obtained under a fixed a_1. In other words, the resonance in Fig. 28 is a bona fide resonance. The NLFM signal is still enhanced and the time-varying characteristic frequency extracted well. Compared with the aperiodic resonance obtained by tuning b_1 parameters, the adaptive aperiodic resonance not only has a better enhancement effect, but also can quickly obtain the optimal parameters.

6. Conclusion

In this work, a new aperiodic resonance phenomenon in a nonlinear system excited by NLFM signal is realized by a piecewise re-scaled method. Different types of NLFM signal can be enhanced by the aperiodic resonance. The validity of this method is first verified by constructing several kinds of NLFM signal. The method can also be used in a noise background. Then, the above results are verified once again by experimental vibration signals corresponding to bearing fault under variable speed condition. The method cannot only enhance signal, but also remove noise and interference components. It provides a reference in processing the non-stationary signal in some real engineering occasions. In order to select system parameters to induce an optimal system resonance quickly, an adaptive piecewise re-scaled aperiodic resonance method is further put forward. With the help of the QPSO algorithm, the problem of optimal parameters selection is solved excellently. Meanwhile, compared with the results obtained without using the QPSO algorithm, this method has a much better enhancement effect. The adaptive aperiodic resonance obtained by the optimization algorithm is a bona fide resonance.

Differently as what happens with the famous SR or VR, besides the single external characteristic signal, there is no other auxiliary signal or noise. It is only necessary to select appropriate system parameters under the single external excitation to induce a strong resonance. This constitutes a new result in the paper, especially for NLFM signal excitation case.

Declaration of Competing Interest

None.

CRediT authorship contribution statement

Jianhua Yang: Conceptualization, Writing - review & editing, Funding acquisition. **Shuai Zhang:** Writing - original draft, Formal analysis. **Miguel A.F. Sanjuán:** Writing - review & editing, Funding acquisition. **Houguang Liu:** Formal analysis.

Acknowledgments

Jianhua Yang acknowledges financial support by the Fundamental Research Funds for the Central Universities (Grant No. 2019GF04) and the Priority Academic Program Development of Jiangsu Higher Education Institutions. Miguel A F Sanjuán acknowledges the Spanish State Research Agency (AEI) and the European Regional Development Fund (FEDER) under Project No. FIS2016-76883-P.

References

[1] Manwar R, Hosseinzadeh M, Hariri A, Kratkiewicz K, Noei S, Avanaki MRN. Photoacoustic signal enhancement: towards utilization of low energy laser diodes in real-time photoacoustic imaging. Sensors 2018;18(10):3498.
[2] Rayner PJ, Duckett SB. Signal amplification by reversible exchange (SABRE): from discovery to diagnosis. Angew Chemie Int Ed 2018;57(23):6742–53.
[3] Liu C, Dong J, Waterhouse GIN, Cheng ZQ. Electrochemical immunosensor with nanocellulose-Au composite assisted multiple signal amplification for detection of avian leukosis virus subgroup. J Biosens Bioelectron 2018;101:110–15.
[4] Lei B, Wang J, Li J, Tang J, Wang YS, Zhao W, Duan YX. Signal enhancement of laser-induced breakdown spectroscopy on non-flat samples by single beam splitting. Opt Express 2019;27(15):20541–57.
[5] Repenko T, Rix A, Nedilko A. Strong photoacoustic signal enhancement by coating gold nanoparticles with melanin for biomedical imaging. Adv Funct Mater 2018;28(7):1705607.
[6] Li Y, Tian D, Ding Y, Yang G, Liu K. A review of laser-induced breakdown spectroscopy signal enhancement. Appl Spectrosc Rev 2018;53(1):1–35.
[7] Zhang X, Wang JX, Liu Z, Wang JL. Weak feature enhancement in machinery fault diagnosis using empirical wavelet transform and an improved adaptive bistable stochastic resonance. ISA Trans 2019;84:283–95.
[8] Ren BY, Hao YS, Wang HQ, Song LY, Gang Tang, Yuan HF. A sparsity-promoted method based on majorization-minimization for weak fault feature enhancement. Sensors 2018;18(4):1003.
[9] Gan M, Wang C, Zhu C. Fault feature enhancement for rotating machinery based on quality factor analysis and manifold learning. J Intell Manuf 2018;29(2):463–80.
[10] Laureti S, Silipigni G, Senni L, Tomasello R, Burrascano P, Ricci M. Comparative study between linear and non-linear frequency-modulated pulse-compression thermography. Appl Optics 2018;57(18):D32–9.
[11] Hao H. Multi component LFM signal detection and parameter estimation based on EEMD–FRFT. Optik 2013;124(23):6093–6.
[12] Bi G, Li X, See CMS. LFM signal detection using LPP-Hough transform. Signal Process 2011;91(6):1432–43.
[13] Widyantara MR, Suratman FY, Widodo S, Daud P. Analysis of non linear frequency modulation (NLFM) waveforms for pulse compression radar. J Elektron Telekom 2018;18(1):27–34.
[14] Saeedi J, Faez K. Synthetic aperture radar imaging using nonlinear frequency modulation signal. IEEE T Aero Elec Sys 2016;52(1):99–110.

[15] Zhao Y, Ritchie M, Lu XY, Su WM, Gu H. Non-continuous piecewise nonlinear frequency modulation pulse with variable sub-pulse duration in a Mimo Sar radar system. Remote Sens Lett 2020;11(3):283–92.
[16] Yi M, Huang J, Ma Y. An efficient echo cancelling scheme based on NTH-order SSC algorithm for nonlinear frequency modulated signal. Optik 2017;149:229–38.
[17] Dantas TM, Costa-Felix RPB, Machado JC. Nonlinear frequency modulated excitation signal and modified compressing filter for improved range resolution and side lobe level of ultrasound echoes. Appl Acoust 2018;130:238–46.
[18] Feng ZP, Chen XW, Wang TY. Time-varying demodulation analysis for rolling bearing fault diagnosis under variable speed conditions. J Sound Vib 2017;400:71–85.
[19] Chen SQ, Yang Y, Dong XJ, Xing GP, Peng ZK. Warped variational mode decomposition with application to vibration signals of varying-speed rotating machineries. IEEE T Instrum Meas 2018;99:1–13.
[20] Li C, Sanchez V, Zurita G, Lozada MC, Cabrera D. Rolling element bearing defect detection using the generalized synchrosqueezing transform guided by time–frequency ridge enhancement. ISA Trans 2016;60:274–84.
[21] Mishra C, Samantaray AK, Chakraborty G. Rolling element bearing defect diagnosis under variable speed operation through angle synchronous averaging of wavelet de-noised estimate. Mech Syst Signal Process 2016;72:206–22.
[22] Lin LF, Yu L, Wang H, Zhong S. Parameter-adjusted stochastic resonance system for the aperiodic echo chirp signal in optimal FRFT domain. Commun Nonlinear Sci Numer Simulat 2017;43:171–81.
[23] Lin L, Wang H, Lv W. Stochastic resonance system with linear random frequency fluctuation for aperiodic LFM signal. Nonlinear Dyn 2017;88(2):1361–71.
[24] Staszewski WJ, Worden K, Tomlinson GR. Time-frequency analysis in gearbox fault detection using the Wigner–Ville distribution and pattern recognition. Mech Syst Signal Process 1997;11(5):673–92.
[25] Rajagopalan S, Restrepo JA, Aller JM, Habetler TG, Harleyet RG. Nonstationary motor fault detection using recent quadratic time-frequency representations. IEEE T Ind Appl 2008;44(3):735–44.
[26] Gammaitoni L, Hänggi P, Jung P, Marchesoni F. Stochastic resonance. Rev Mod Phys 1998;70(1):223.
[27] Landa PS, McClintock PVE. Vibrational resonance. J Phy A 2000;33(45):L433.
[28] Lu SL, He QB, Kong FR. Effects of underdamped step-varying second-order stochastic resonance for weak signal detection. Digit Signal Process 2015;36:93–103.
[29] Han D, An S, Shi P. Multi-frequency weak signal detection based on wavelet transform and parameter compensation band-pass multi-stable stochastic resonance. Mech Syst Signal Process 2016;70:995–1010.
[30] Kumar S, Jha RK. Weak signal detection using stochastic resonance with approximated fractional integrator. Circuits Syst Signal Process 2019;38(3):1157–78.
[31] Huang DW, Yang JH, Zhou DJ, Sanjuán MAF, Liu HG. Recovering an unknown signal completely submerged in strong noise by a new stochastic resonance method. Commun Nonlinear Sci Numer Simulat 2019;66:156–66.
[32] Liu HG, Liu XL, Yang JH, Sanjuán MAF, Cheng G. Detecting the weak high-frequency character signal by vibrational resonance in the Duffing oscillator. Nonlinear Dyn 2017;89(4):2621–8.
[33] Xiao L, Zhang XH, Lu SL, Xia TB, Xi LF. A novel weak-fault detection technique for rolling element bearing based on vibrational resonance. J Sound Vib 2019;438:490–505.
[34] Jia PX, Wu CJ, Yang JH, Sanjuán MAF, Liu GX. Improving the weak aperiodic signal by three kinds of vibrational resonance. Nonlinear Dyn 2018;91(4):2699–713.
[35] Jia PX, Yang JH, Zhang X, Sanjuán MAF. On the LFM signal improvement by piecewise vibrational resonance using a new spectral amplification factor. IET Signal Process 2018;13(1):65–9.
[36] Zhang XF, Hu NQ, Cheng Z, Hu L. Enhanced detection of rolling element bearing fault based on stochastic resonance. Chin J Mech Eng 2012;25(6):1287–97.
[37] Leng YG, Wang TY. Numerical research of twice sampling stochastic resonance for the detection of a weak signal submerged in a heavy noise. Acta Phys Sin 2003;52:2432–7.
[38] Tan JY, Chen XF, Wang JY, Chen HX, Cao HR, Zi YY, He ZJ. Study of frequency-shifted and re-scaling stochastic resonance and its application to fault diagnosis. Mech Syst Signal Process 2009;23(3):811–22.
[39] Leng YG, Leng YS, Wang TY, Guo Y. Numerical analysis and engineering application of large parameter stochastic resonance. J Sound Vib 2006;292(3–5):788–801.
[40] Huang DW, Yang JH, Zhang JL, Liu HG. An improved adaptive stochastic resonance method for improving efficiency of bearing faults diagnosis. P I Mech Eng C: J Mec 2018;232(13):2352–68.
[41] Wu C, Wang Z, Yang J, Sanjuán MAF. Adaptive piecewise re-scaled stochastic resonance excited by the LFM signal. Eur Phys J Plus 2020;135(1):130.
[42] Xu YF, Gao J, Chen GC, Yu J. Quantum particle swarm optimization algorithm. Appl Mech Mater 2011;63:106–10.